Complex coordination of multi-scale cellular responses to environmental stress†‡

Luís L. Fonseca,[ab] Claudia Sánchez,[a] Helena Santos[a] and Eberhard O. Voit*[b]

Received 13th July 2010, Accepted 12th October 2010
DOI: 10.1039/c0mb00102c

Cells and organisms are regularly exposed to a variety of stresses, and effective responses are a matter of survival. The article describes a multi-scale experimental and dynamical modeling analysis that clearly indicates concerted stress control in different temporal and organizational domains, and a strong synergy between the dynamics of genes, proteins and metabolites. Specifically, we show with *in vivo* NMR measurements of metabolic profiles that baker's yeast responds to a paradigmatic stress, heat, at three organizational levels and in two time regimes. At the metabolic level, an almost immediate response is mounted. However, this response is a "quick fix" in comparison to a much more effective response that had been pre-organized in earlier periods of heat stress and is an order of magnitude stronger. Equipped with the metabolic profile data, our modeling efforts resulted in a crisp, quantitative separation of response actions at the levels of metabolic control and gene regulation. They also led to predictions of necessary changes in protein levels and clearly demonstrated that formerly observed temperature profiles of key enzyme activities are not sufficient to explain the accumulation of trehalose as an immediate response to sudden heat stress.

Introduction

Cells and organisms respond to environmental stresses with a multitude of defense mechanisms that rely on action and control throughout the hierarchy of biological organization, from genes and proteins to signaling processes and changes in profiles of large and small metabolites. The complexity of these responses suggests a two-pronged systems biological approach that combines *de novo* experimental and computational modeling. Here, we present such an approach with the goal of elucidating the coordination of complex multi-scale responses in the baker's yeast *Saccharomyces cerevisiae* to a paradigmatic environmental stress: heat. Within minutes of the initiation of heat stress, transcription factors are mobilized and translocated, and numerous genes respond with strong changes in expression.[1–3] Heat shock proteins dramatically increase in prevalence, and the profile of sphingolipids changes and in turn affects gene expression in a controlled fashion.[4,5] Finally, heat induces the synthesis of small molecules and, in particular, the disaccharide trehalose, which in yeast can account for up to 40% of the total cell mass under heat stress.[6]

The accumulation of trehalose points to its crucial role as protector of cell components against the damaging effects of heat. In particular, it acts as an inhibitor of protein aggregation at elevated temperatures,[7] and cells defective in the synthesis of trehalose are highly thermo-sensitive.[8] Targeted DNA-microarray experiments have demonstrated that transcript levels of genes associated with the trehalose pathway change within a few minutes of temperature jumps and may last for over one hour.[1,9,10] This observation has been interpreted as an indication that the heat response is primarily controlled at the genomic level. However, there is a growing stream of evidence pointing to the importance of fast changes in the levels of metabolites, their effects on enzyme activities, and mechanisms of cell adaptation to the suboptimal environmental changes. These findings suggest that the heat stress response is a systemic phenomenon that should therefore be analyzed with methods of systems analysis. If control is indeed shared, insights into the multi-level coordination of the heat response will lead to a deeper understanding of a complex, paradigmatic cellular regulation task. On the more practical side, these insights will be useful for the generation of yeast strains that are better capable of withstanding adverse conditions.

The heat stress response contains several aspects that are not intuitive and will be addressed with our systemic analysis. First, there is clear evidence that the genes coding for both trehalose synthesis and degradation, namely trehalose 6-phosphate synthase (TPS1), trehalose 6-phosphate phosphatase (TPS2) and trehalase (NTH1/2 and ATH1), are strongly up-regulated under high temperature conditions. This regulatory design is intriguing because it seems to suggest the operation of a futile cycle under heat stress.[6] Second, the up-regulation of trehalase is counterintuitive, since it seems to hasten the degradation of a metabolite that is in dire need. Third, this up-regulation

[a] *Instituto de Tecnologia Química e Biológica, Universidade Nova de Lisboa, 2780-156 Oeiras, Portugal*
[b] *Integrative BioSystems Institute and The Wallace H. Coulter Department of Biomedical Engineering, Georgia Institute of Technology, 313 Ferst Drive, Suite 4103, Atlanta, GA 30332-0535, USA. E-mail: eberhard.voit@bme.gatech.edu; Tel: +1 (404) 385-5057*

† Authors' contributions: LLF and CS executed all lab experiments. LLF and EOV performed the modeling. HS supervised all experimental aspects. LLF wrote the first draft of the manuscript, and HS and EOV contributed to writing and editing.

‡ Electronic supplementary information (ESI) available: Supplementary details. See DOI: 10.1039/c0mb00102c

counteracts the unambiguously documented increases in the activity of trehalose producing enzymes and the decrease in trehalase activity under heat conditions.[11] Finally, it is a challenge to assess objectively whether the reported changes in enzyme activities[11] are by themselves sufficient for mounting an effective response. Our analysis will answer these questions.

The main set of experiments presented here consisted of the on-line tracing of metabolite dynamics in two groups of yeast cells, using ^{13}C-NMR spectroscopy *in vivo*.[12] One group of cells was grown at optimal temperature (T = 30 °C) and the other adapted to growth at a supra-optimal temperature (T = 39 °C). For each experiment, the temperature was initially set to 30 °C (control condition) and a first pulse of 65 mM ^{13}C-labeled glucose was given. Once glucose was depleted, the temperature of the cell suspension was rapidly increased to 39 °C (heat stress condition) and a second glucose pulse was added. Subsequently the temperature was returned to the optimal 30 °C (recovery condition). This experimental approach allowed us to separate the direct effect of temperature on enzyme activity from the long-term effect of heat-induced changes in protein levels. Each experiment resulted in metabolic time courses, which we analyzed with a newly devised computational systems model. In both groups of cells, the overall response patterns were similar, but the different conditions during growth led to quantitatively very distinct metabolic profiles.

Results

Experimental results

Metabolite dynamics in cells grown at 30 °C. As a representative result, Fig. 1 shows the metabolic time series of [1-^{13}C]glucose consumption, accumulation of trehalose and fructose 1,6-bisphosphate (FBP), and release of end-products (ethanol, acetate and glycerol) in cells grown under optimal conditions (30 °C). The results clearly reflect the metabolic responses to the three pulses of [1-^{13}C]glucose at times t = 5 (30 °C), t = 48 (39 °C), and t = 75 (30 °C).

Analysis of glucose consumption showed that heat stress increased the glucose transport capacity up to 25 ± 5% over baseline (see ESI‡). Upon return to 30 °C (recovery conditions), the glucose transport capacity returned to 96 ± 4% of the control.

The trehalose pool increased rapidly, concomitantly with glucose consumption. In response to the first glucose pulse, FBP and trehalose accumulated transiently to 18 ± 2 and 4.8 ± 0.8 mM, respectively. In response to the second pulse (heat-stress condition), trehalose accumulation was more than twice as high (9.8 ± 1.2 mM) and the rate of trehalose degradation was significantly lower.

Under recovery conditions, trehalose accumulation was comparable to that observed under control conditions and exhibited a similar dynamics. We confirmed that trehalose was located inside the cell and no evidence was found for secretion of this sugar to the external medium. We also refuted the hypothesis that the increase in the pool of trehalose could be due to an increase in the size of the glucose 6-phosphate (G6P) pool (see ESI‡).

Targeted experiments with a constant glucose supply demonstrated that trehalose accumulation begins within 2 min of heat stress (see ESI‡). This finding is intriguing because such a fast response cannot be dependent on transcriptional or translational regulation processes, which typically occur at a time scale of about 15 min.[11] Instead, the response is apparently the result of a direct effect of temperature on the activity of the enzymes that are responsible for the synthesis and degradation of trehalose. We will return to this aspect later.

The newly formed trehalose was slowly degraded once the glucose bolus was used-up, both at 30 °C and 39 °C (Fig. 1). This trehalose degradation process was clearly dependent on the ambient temperature with rates of 37 μmol h^{-1} g^{-1} dry

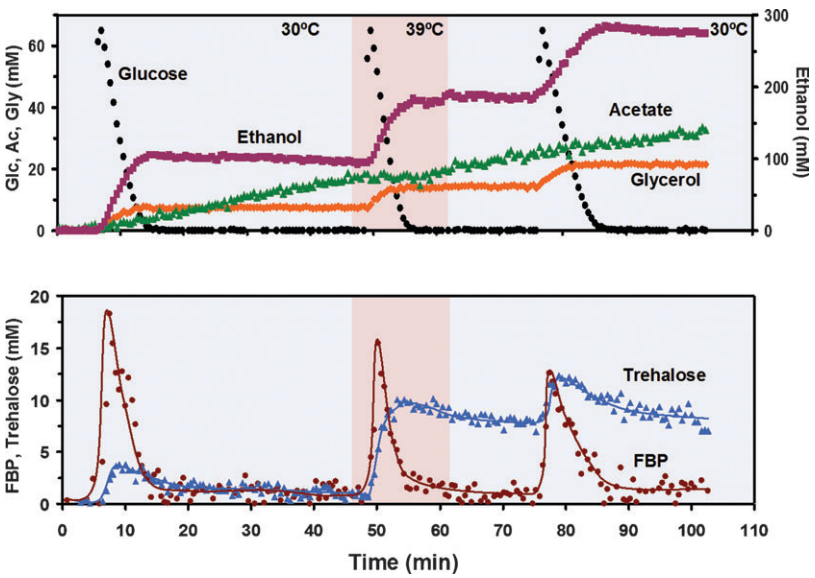

Fig. 1 Metabolite time courses of glucose metabolism determined by *in vivo* ^{13}C-NMR in *Saccharomyces cerevisiae* grown under optimal temperature. Three consecutive pulses of glucose were supplied under different temperatures: 30 °C ( ); 39 °C ( ); and back to 30 °C. Experimental data are shown for glucose (●) ethanol (■), glycerol (◆), acetate (▲), FBP (●) and trehalose (▲).

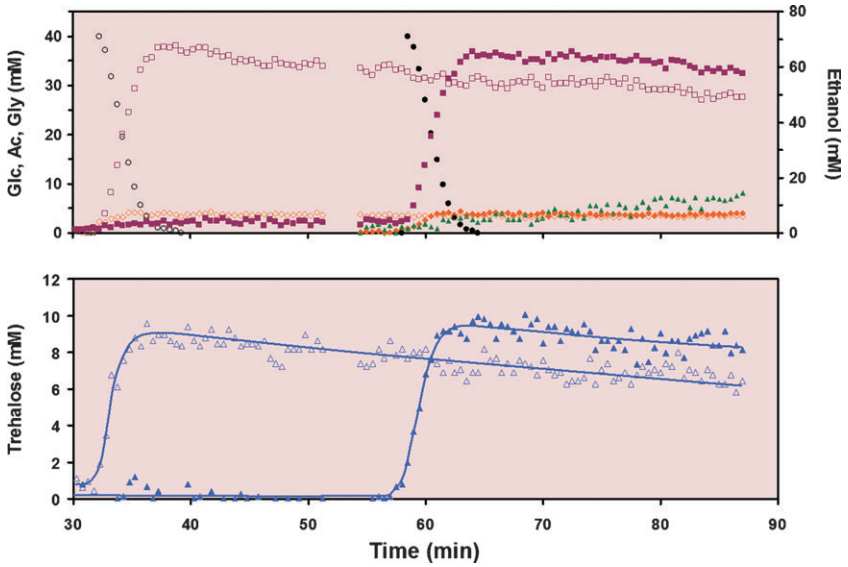

Fig. 2 Metabolite time courses of glucose metabolism determined by *in vivo* ^{13}C-NMR in *Saccharomyces cerevisiae* grown under optimal temperature. Prior to time 0 the cells were supplied with unlabeled glucose at 30 °C, to keep the experimental design similar to the other experiments. Then, the temperature was increased to 39 °C and two pulses of glucose were supplied ([2-^{13}C]glucose and [1-^{13}C]glucose, respectively). All metabolites produced from [2-^{13}C]glucose are shown in open symbols, while metabolites produced from [1-^{13}C]glucose are shown in solid symbols. Acetate produced from [2-^{13}C]glucose is not shown due to its inherently low NMR visibility (under the conditions used). The metabolism of [2,2′-$^{13}C_2$]trehalose (derived from [2-^{13}C]glucose) seems to be unaffected by the uptake and degradation of [1-^{13}C]glucose and consequent accumulation of [1,1′-$^{13}C_2$]trehalose. It appears as if the two isotopomers of trehalose are degraded independently of each other (see ESI‡ for a possible explanation). Experimental data are shown for glucose (●,○) ethanol (■,□), glycerol (◆,◇), acetate (▲) and trehalose (▲,△).

mass at 30 °C *versus* 20 μmol h^{-1} g^{-1} dry mass at 39 °C, respectively. These results are consistent with the reported inactivation of trehalase at elevated temperatures.[11]

To obtain deeper insight into this hydrolysis step, we performed experiments where the exposure of cells to 39 °C was extended and a second glucose pulse was added. To distinguish the individual trehalose pools in the NMR spectra, different glucose isotopomers were supplied in the first and second pulses, *i.e.*, [2-^{13}C]glucose and [1-^{13}C]glucose, respectively (see Fig. 2). Surprisingly, the degradation profile of trehalose derived from the first pulse was almost perfectly linear and continued apparently unaffected by the additional trehalose deriving from the second pulse. Furthermore, the second pulse led to the same linear trehalose degradation profile as the first, and the two degradation processes ran quasi in parallel. This distinction between trehalose from different pulses also seems to be present during recovery in the experiments described before (see Fig. 1) where it appears that the "new" trehalose from the third bolus is degraded more quickly, whereas the degradation profile of the "old" trehalose (second bolus) seems to follow the trend that began during heat stress, irrespective of the third pulse. At present, no definite explanation can be given for this apparent independence of trehalose from different pulses; however, the ESI‡ discuss this observation further and analyze a possible hypothesis.

Metabolite dynamics in heat adapted cells. In order to study the long-term effects of heat treatment, we subjected the cells to a supra-optimal temperature (39 °C) during the final 40 min of growth prior to the *in vivo* NMR experiments. As before, three glucose pulses (65 mM) were administered to these

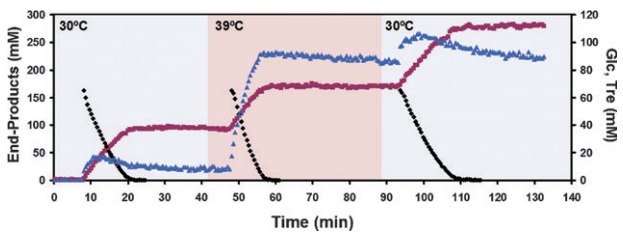

Fig. 3 Metabolite time courses of glucose metabolism by heat-adapted *Saccharomyces cerevisiae* as measured by *in vivo* ^{13}C-NMR. Cells were derived from a culture exposed to 39 °C during the last 40 min of growth. Three consecutive pulses of glucose (●) were supplied under different temperatures: 30 °C ( ); 39 °C ( ); and back to 30 °C. Trehalose (▲) accumulated intracellularly; the sum of released end-products (■, ethanol, glycerol and acetate) is shown. FBP was below the detection level.

heat-adapted cells and the metabolite responses were analyzed by ^{13}C-NMR as before. Trehalose accumulated to 16.7 ± 2 mM under control conditions (30 °C) and to 93.1 ± 5 mM under heat-stress conditions (39 °C) (Fig. 3). These values compare to 4.8 and 9.8 mM, respectively, for cells grown under optimal temperature (Fig. 1). This increase of almost an order of magnitude in trehalose synthesis clearly shows the extent of changes in gene expression induced during adaptation to heat stress. Interestingly, the level of FBP in these cells was below the detection limit of approximately 1 mM in our methodology.

Modeling results. The primary purposes of the modeling effort were two-fold. First, we intended to answer the question of whether the temperature profiles of enzyme activities as

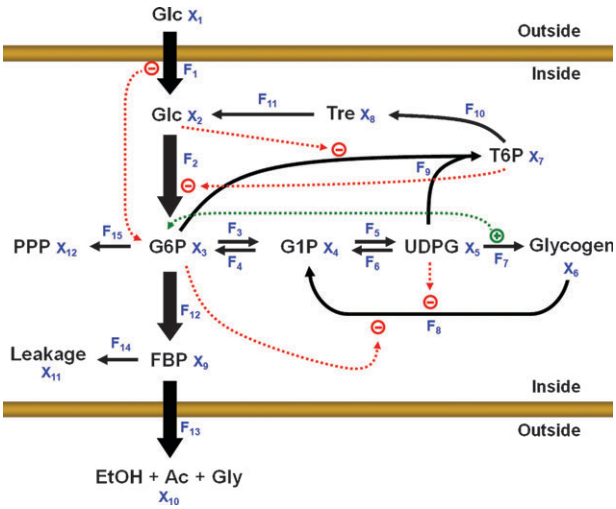

Fig. 4 Schematic representation of *Saccharomyces cerevisiae* glycolysis and trehalose cycle reactions used in the model. X_i and F_i represent the dependent variables of the model and the fluxes, respectively. Inhibitory interactions are shown in red, while activation of glycogen synthase by glucose 6-phosphate is indicated in green. Abbreviations: X_1, extracellular glucose; X_2, intracellular glucose; X_3, glucose 6-phosphate; X_4, glucose 1-phosphate; X_5, UDP-glucose; X_6, glycogen; X_7, trehalose 6-phosphate; X_8, trehalose; X_9, fructose 1,6-bisphosphate; X_{10}, extracellularly accumulated end-products (ethanol, acetate and glycerol); X_{11}, glucose consumed by other pathways (*e.g.*, TCA); X_{12}, glucose diverted to the pentose phosphate pathway; F_1, glucose transport; F_2, glucokinase; F_3 and F_4, phosphoglucomutase (forward and reverse); F_5 and F_6, glucose 1-phosphate uridylyltransferase (forward and reverse); F_7, glycogen synthase; F_8, glycogen phosphorylase; F_9, trehalose 6-phosphate synthase; F_{10}, trehalose 6-phosphate phosphatase; F_{11}, trehalase; F_{12}, phosphoglucose isomerase and phosphofructokinase; F_{13}, aggregated step of all enzymatic steps between fructose 1,6-bisphosphate aldolase and the release of end-products; F_{14}, flux towards other pathways; F_{15}, flux into the pentose phosphate pathway.

reported by Neves and François[11] (ESI‡ Fig. S3) are sufficient to explain the accumulation of trehalose as an immediate response to sudden heat stress. Second, the model was designed to predict heat-induced changes at the protein level from the metabolic time series data obtained with heat-adapted cells.

As our modeling framework, we used a Generalized Mass Action (GMA) representation, which we designed according to the rules of Biochemical Systems Theory (BST[13–16]). The base model was subsequently augmented with temperature-dependent modifiers, as discussed in the Methods section. The structure of the model (Fig. 4) comprises the upper part of glycolysis and the trehalose cycle, *i.e.*, trehalose synthesis and degradation. The carbon flux toward the pentose phosphate pathway (PPP) was considered as well. Experiments specifically elucidating this branch showed that the PPP flux has a magnitude of 5% of the glycolytic flux under both optimal and heat stress conditions (see ESI‡). A "leakage" flux (F_{14}) was included to account for carbon channeled to other routes, such as the TCA cycle and respiration.

The direct effect of temperature on enzyme performance was modeled using temperature coefficients (Q_{10}) and the heat-induced changes in protein levels were modeled with a step function. Specifically, we included in each flux an indicator variable τ. For cells grown under optimal conditions, this indicator was set to $\tau = 1$, while it was defined as $\tau = 2$ for heat-adapted cells. Changes in protein amounts due to increased gene expression were subsequently modeled as factors τ^{p_i}. We chose this format to facilitate comparisons with changes in expression reported in the literature, which are typically given as powers of 2.

The data from the first two pulses of glucose, supplied to cells grown at optimal temperature (Fig. 1), were used to parameterize the model. In this situation, all proteins were per definition expressed at their baseline values ($\tau = 1$). The data from the first two pulses of glucose supplied to heat-adapted cells (Fig. 3) were used to estimate the changes in protein content (P_i). As the results indicate, the model fits the data rather well under all four conditions (Fig. 5).

Parameter estimates. The temperature coefficients for the enzymes producing and degrading trehalose were obtained from an article by Neves and François,[11] who studied the temperature dependence of the activity of trehalose 6-phosphate synthase, trehalose 6-phosphate phosphatase, and neutral trehalase. We smoothed these data (ESI‡ Fig. S3) and obtained from the smoothed curves direct estimates of the corresponding temperature coefficients, namely, $Q_9 = 2.48$, $Q_{10} = 2.35$ and $Q_{11} = 0.42$.

Results of inverse estimations from the metabolic time series data provided all BST parameters (kinetic orders and rate constants; see Methods), as well as the remaining temperature coefficients (Q_1, Q_3, Q_{13}) and the heat induced changes in protein levels (P_i). These parameter values are presented in Tables 1, S1 and S2.‡ Model diagnostics demonstrated that the model with these parameter values was stable and robust (see ESI‡).

A comparison of the degree of temperature dependence inferred here with previously published data[1,2,17] shows that they are generally in good agreement (Tables 1 and S2‡). This agreement is most easily seen for published enzyme or protein data. However, because such data are not available for all fluxes in Table 1, we also included published expression data (mRNA levels) as substitutes. For example, the model predicted that heat-adapted cells have a lower amount of glucose transporters (70% of that in control cells), which is similar to the reduced glucose transport that was observed in steady-state chemostat cultures grown at 30 °C or 38 °C.[2] In this reported case, the transport was reduced to about 70–80%, depending on the temperature at which the assays were performed. Also, most of the changes determined by Gasch and collaborators[1] for the mRNA levels of yeast cells that were heat stressed from 25 °C to 37 °C are in reasonable agreement with our results: Table 1 compares our results with Gasch's measurements at time 15 min, where the deviation of gene expression from baseline is maximal.

The model made predictions regarding the dynamics of glycogen that are partially in agreement with literature information. For instance, the model predicted only a modest increase in glycogen synthesis and a strong increase in glycogen phosphorylase. While the latter is comparable to a value reported earlier,[17] the former is clearly different. The

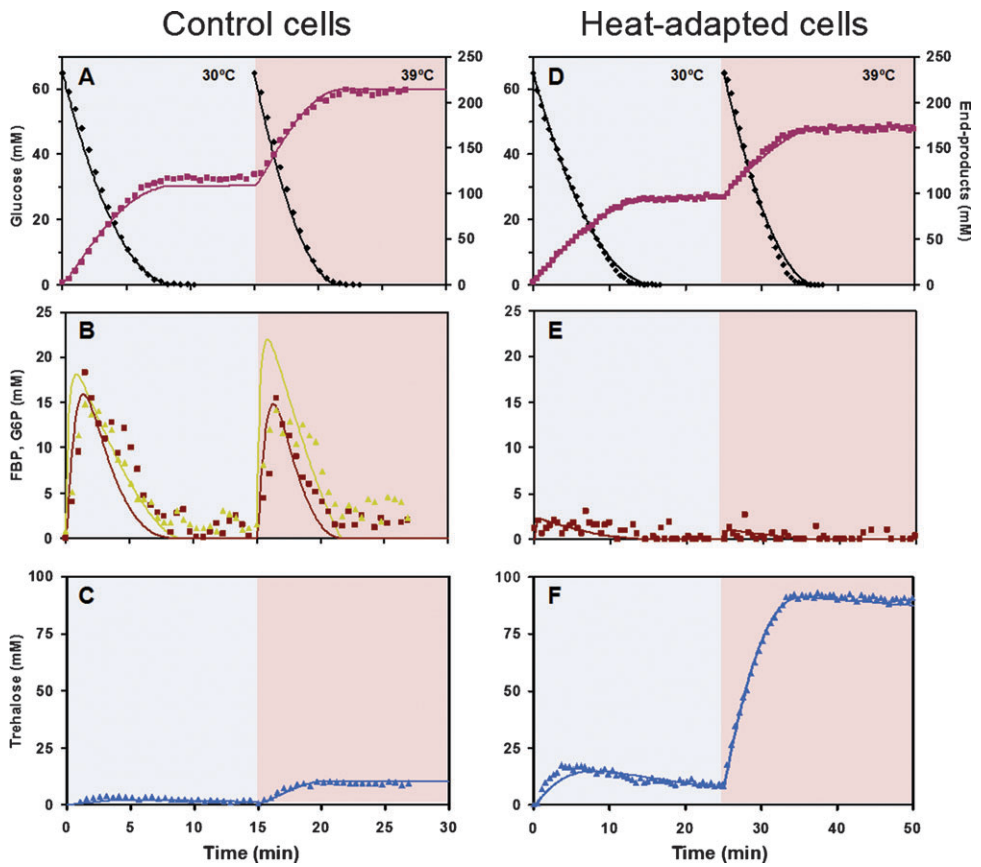

Fig. 5 Model simulation of the experimental data obtained with control cells and heat-adapted cells. Symbols show experimental data obtained with cells grown at 30 °C (panels A, B, C), and cells subjected to 39 °C during the last 40 min of growth (panels D, E, F). Cells were supplied with consecutive glucose pulses at 30 °C and at 39 °C. The lines show the simulated values obtained with the model. Temperatures: 30 °C ( ) and 39 °C ( ). Panels A and D: glucose (X_1,◆) and end-products (X_{10}, ■). Panels B and E: G6P (X_3, ▲) and FBP (X_9, ■). Panels C and F: trehalose (X_8, ▲).

Table 1 Comparison of protein changes that were computationally inferred for heat adapted cells (grown at 39 °C for 40 min before harvesting) with data from the literature

Flux	Model step	Fold change (2^{Pi})	mRNA change (15 min)[a]	Weighted mRNA change[b]	Change in enzyme activity or protein level
1	HXT	0.7			0.8[c]
2	HXK	9.2	5.7 (HXK1) 0.6 (HXK2) 5.3 (HXK3)	8	1.4[c]
3	PGM^F	20.7	0.06	16	
4	PGM^R	17.3	7.2		
5	UGP^F	16.2		16	
6	UGP^R	26.0			
7	GSY	0.9	4.0	16	7.4[d]
8	GPH	61.8	6.8	50	5.5[d]
9	TPS1	21.5	12.9	12	4.0[d]
10	TPS2	14.2	17.9	18	
11	NTH	4.9	11.5	6	3.0[e]
12	PFK + PGI	1.0			1.1[c]
13	"FBA"	1.2	0.4	1	(0.7–2.8)[c,f]
14	Leakage	4.1	1.8		
15	ZWF	1.0	2.3	6	

[a] From ref. 1. [b] Weighted values for isozyme activities and mRNA copy numbers ref. 17. [c] From ref. 2. [d] From ref. 42. [e] From ref. 43. "FBA" designates the collection of enzymatic steps between fructose 1,6-bisphosphate aldolase (FBA) and the release of end-products; [f] Range of values reported for all the enzymatic activities after FBA.

main reason is presumably that glycogen is a complicated polymer whose dynamics is difficult to model, because the addition or removal of monomers does not really change its concentration, but rather its size. Furthermore, our experimental methods did not allow us to measure glycogen directly. As a substitute, we analyzed the effects of artificially changing the dynamics of this metabolite and found that the system is essentially unaffected, with the notable exception of the amount of glycogen itself. Because our experimental methods do not allow us to validate the model with respect to glycogen, we cannot say to what degree glycogen accumulates under our experimental conditions.

Beyond the effects on the trehalose associated enzymes reported by Neves and François,[11] our model predicted direct effects of temperature on other protein activities, namely glucose transport and FBP consumption, as well as phosphoglucomutase. Postmus and collaborators[2] discovered a small increase (around 10%) in the transport of glucose and a 1.3-fold increase in the activity of the fructose 1,6-bisphosphate aldolase (FBA) (Table S2‡). This latter value is similar to our model prediction, although it is not directly comparable, because our value does not represent the activity of this enzyme alone, but represents the collection of all enzymatic steps between FBP and the release of ethanol, glycerol and acetate.

Immediate and long-term responses to elevated temperature. Since each pulse of glucose was supplied to non-growing cells at different temperatures (30 °C, 39 °C), it was possible to extract from control cells the direct effect of temperature on the system, and to characterize it in the form of temperature coefficients. Concurrently using the data acquired with heat-adapted cells, it was possible to calculate by how much the level of each protein changed (Table 1).

As a thought experiment, we took the temperature dependence of enzyme activities observed by Neves and François[11] at face value (outside simple smoothing) and considered no other effects of heat. The model with these settings demonstrated trends in the right direction, but the results also showed clearly that these alterations in enzyme activities are insufficient to mount the observed response (Fig. 6). The most noticeable discrepancies are apparent in the extent of trehalose accumulation and the kinetics of glucose consumption at 39 °C. In response to this situation, we explored computationally which other enzymes would have to be temperature dependent beyond the direct effects on

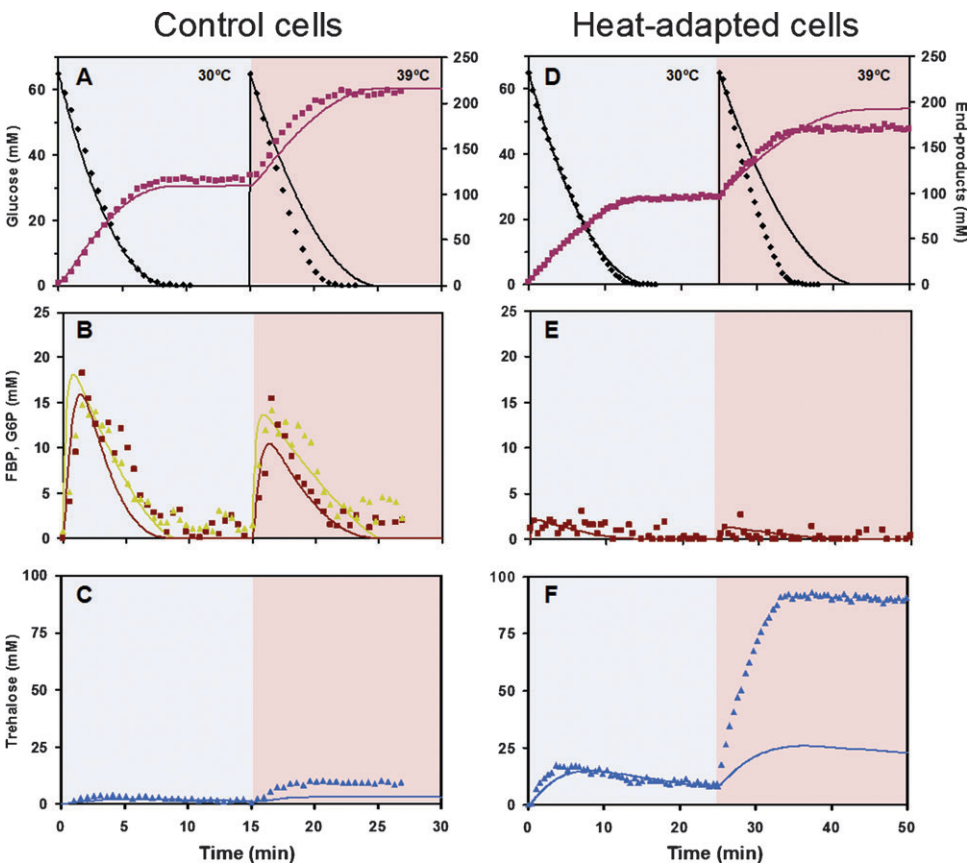

Fig. 6 Direct effects of temperature on the activities of the three enzymes implicated in trehalose metabolism[11] are not sufficient to simulate the experimental metabolic responses to heat stress in control cells and heat-adapted cells adequately. Lines show simulation results. Symbols are experimental data obtained with cells grown at 30 °C (panels A, B, C), and cells subjected to 39 °C during the last 40 min of growth (panels D, E, F). Cell suspensions were supplied with consecutive glucose pulses at 30 °C and at 39 °C. Temperatures: 30 °C ( ) and 39 °C ( ). Panels A and D: glucose (X_1,◆) and end-products (X_{10}, ■). Panels B and E, G6P (X_3, ▲) and FBP (X_9, ■). Panels C and F: trehalose (X_8, ▲).

trehalose related enzymes. As a minimal set of additional changes in enzyme activities, we found that temperature dependences in glucose uptake and FBP removal, along with a postulated change in phosphoglucomutase, permitted accurate fits to all scenarios tested (Fig. 5). Of course, good model fits can also be obtained with larger subsets of temperature dependent proteins, spread throughout the network, but it seemed worthwhile identifying a "minimal" model for temperature dependencies, where three strong dependencies turned out to be sufficient to capture all observed scenarios with sufficient accuracy.

The model was able to simulate the metabolic behavior of cells grown under control conditions, as well as of cells preconditioned by heat during growth, just by taking into consideration the heat induced changes in protein levels. These results, together with the experimental measurements, confirm that the immediate trehalose response to heat is regulated at the protein level, where the catalytic rates of key enzymes change upon increases in temperature. These changes may be explainable with the Arrhenius effect and thermal dependence of the protein structure. This finding is intriguing, because attention to metabolic regulation has been dwarfed in the literature by a dominant focus on genomic regulation.

Discussion

The heat stress response in yeast comes close to an ideal paradigm for forays into discovering how cells coordinate survival tasks. Comparatively speaking, yeast is rather well understood and amenable to experimentation, its trehalose response is massive and almost immediate, and it has been documented that genes, proteins, lipids, and signaling pathways are involved in the concerted efforts of the cell to regain a tolerable internal state that permits it to weather the undesired environmental condition. Although much is known about the heat response, it is still full of surprises. Recognizing its systemic nature, we launched a combined experimental and modeling investigation, in which we generated *de novo* data under tightly controlled conditions, entered these into a dynamic model, and obtained insights not gained before.

For the new experiments, which complemented genomic and metabolic information in the literature, we chose *in vivo* ^{13}C-NMR in a flow-through mode, which allowed us to take advantage of the inherent non-destructive and non-invasive nature of this method. In particular, this approach permits measurements in rather dense time sequence, which here yielded dynamic metabolic profiles of key compounds of the upper glycolytic and trehalose pathways. These data were ideally suited for the construction and parameterization of a fully dynamic model, which allowed us to tease out the various contributions of genes, proteins and metabolites to the heat stress response and to focus on different time scales and on different organizational scales.

We studied four situations, namely the trehalose responses in "naïve" control cells under optimal and heat conditions, and the same responses in cells that had the chance to adapt to heat conditions toward the end of the exponential growth phase. The option of using non-growing cells to study metabolic responses had the advantage that the cells were relieved of growth-related pressures. In other words, glucose metabolism was uncoupled from growth, which simplified the system, and the cells metabolized glucose almost exclusively toward ethanol, glycerol and acetate, and toward trehalose and glycogen, if needed.

For our model design, we postulated two modes of response action, working concurrently but at different time-scales: an immediate direct effect of temperature on the activity of key enzymes, and a slower genomic/proteomic adaptation to heat exposure during the preceding growth phase. The main advantage of setting up such a two-tiered model was that it enabled us to distinguish crisply between these modes, while still being entirely anchored in experimental data.

While the few previous models of the trehalose pathway had been parameterized with *in vitro* data,[17,26,27] our experiments permitted a minimally biased top-down estimation that was custom-tailored to the specific situation and permitted the separate estimation of immediate and genome-based temperature effects on enzyme activities. In particular, we did not allow any of the intrinsic kinetic parameters, characterizing enzyme affinities, to be changed among the four different situations that were experimentally tested and mathematically modeled. Instead, the direct effect was modeled using typical Q_{10} temperature coefficients, while the alterations in enzyme levels were modeled in a binary fashion that reflected the changes induced by heat during growth. Interestingly, most regulatory interactions, except for the inhibition of hexokinase by trehalose 6-phosphate, had negligible impact. To confirm the modest degree of regulation, we analyzed numerous model variants with stronger regulatory interactions. However, the best fitting models always emerged with very low-magnitude regulatory kinetic orders. It is possible that the regulatory effects found *in vitro* do not play a significant role under the experimental *in vivo* conditions in this work.

The combined experimental and computational analysis yielded several interesting insights. Most importantly, the responses to the sudden availability of glucose not only changed under different temperature regimes, but they were distinctly altered if the cells had been exposed to heat earlier in their lives. Thus, if a naïve control cell is suddenly exposed to heat, it uses the best defense that is immediately available, namely a direct temperature-dependent alteration in the activities of key enzymes. Interestingly, the enzymes that had been identified earlier for this purpose (trehalose 6-phosphate synthase, trehalose 6-phosphate phosphatase, and trehalase)[11] turned out to be necessary but not alone sufficient for the required magnitude of response. In addition, glucose uptake and FBP consumption have to be increased, and the model furthermore suggests a slight alteration in phosphoglucomutase. One might surmise that the structure of many proteins is affected by heat, but the enzymes identified earlier, along with glucose uptake and phosphoglucomutase, emerged as the dominant drivers of the response.

Given the result that the cells are able to mount an effective response solely based on temperature dependent changes in enzyme activities, we asked what the specific contribution of gene expression to the heat stress response might be. We

analyzed this question with longer-term studies, which provided a clear answer: Gene regulation appears to be a means of preconditioning the cells for heat stress later in life. Indeed, preconditioned cells in our experiments exhibited a trehalose response that was an entire order of magnitude stronger than unconditioned cells under the same heat stress.

The model allowed us specifically to predict which protein activities had to be altered *via* gene regulation to mount the observed response. It is not possible categorically to exclude alternative profile changes in genes and/or proteins with the same outcome, but the results predicted by the model are very much in line with direct and indirect information reported in the literature, including the numerical values determined for the kinetic parameters. Specifically, the adapted cells consumed glucose at a 30% reduced rate when examined at 30 °C, without accumulating FBP, and showed a 4-fold higher accumulation of trehalose than control cells. More importantly, when the temperature was raised to 39 °C, the heat-adapted cells accumulated trehalose to a level of almost 100 mM. These dramatic changes were made possible through increased enzyme levels within the trehalose cycle and decreased glucose consumption. By contrast, key enzymes in the lower section of the glycolytic pathway were essentially unchanged, a finding that is indirectly supported by studies in *Xenopus*[18–21] that found no significant changes in glyceraldehyde 3-phosphate-dehydrogenase and pyruvate kinase. Overall, our results on genomic enzyme alterations are also in accordance with independent results reported earlier.[10,17]

Postmus *et al.*[2] reported that steady-state yeast cultures in carbon-limited chemostats exhibited a reduced amount of glucose transporters, but a higher accumulation of FBP. By contrast, our cells clearly showed reduced FBP accumulation, a finding that was supported by our model. The difference may be due to the unrelated experimental conditions. In our case, the reduced amount of glucose input leads to a longer glucose consumption period, while the flux beyond FBP is apparently increased (Table S1‡), which may explain the exhaustion of FBP.

Our computational findings, combined with literature information, allow us to speculate on the puzzling observation of trehalase up-regulation under heat stress. There is every indication that the trehalose degrading genes NTH1/2 and ATH are up-regulated several fold upon the initiation of heat stress and that the protein amount is increased as well. These increases, considered in isolation, would suggest an increased degradation of trehalose in times of heat stress. However, from a systems view, it seems that they are indeed compensating (or compensated by) the documented strong temperature dependent decrease in trehalase activity. This simultaneous up- and down-regulation has the effect that only small amounts of trehalose are degraded during heat stress (see Fig. 1–3), but that the cell is ready to degrade trehalose in large amounts as soon as the environmental temperature sinks. Without the dual, compensating mechanism, the cell would have to begin up-regulating trehalase genes after the return to cooler conditions, which would delay the resuming of normality by twenty or thirty minutes. Thus, it seems that the seemingly contradictory battle between two counteracting processes at the gene and protein levels in fact provides the cell with a strong selective advantage.

In summary, the response to heat is organized at two levels. The first is an immediate metabolic response that is governed by changes in the activities of enzymes that directly depend on temperature. This response is apparently sufficient to satisfy the most urgent needs of the cell. If the cells have the opportunity to adapt to heat, response to later heat exposure is almost ten times stronger than in naïve cells. This adaptation response is much slower and governed by alterations at the genomic level.

Materials and methods

Experimental methods

Saccharomyces cerevisiae strain JK93dα was kindly provided by Dr Ashley Cowart, Medical University of South Carolina. Stock cultures were prepared from shake-flask cultures: 80 ml of YPD medium (yeast extract 10 g l^{-1}, peptone 20 g l^{-1} and dextrose 20 g l^{-1}) in 250 ml flask, grown overnight. Flasks were inoculated to a final OD_{600} of 0.05 and cells were allowed to grow for 18 h at 30 °C with a stirrer speed of 200 RPM. Culture samples were stored in sterile vials at −80 °C as 1 ml aliquots containing 20% glycerol. Further details are presented in the ESI.‡

All *in vivo* NMR experiments were executed as described generically in ref. 12 and specifically in the ESI.‡

The time course experiments were replicated three to five times. Due to the nature of these experiments, it is not feasible to show the variability between the results as error bars in the figures, because each *in vivo* NMR experiment depends on the amount of biomass present in the suspension and must be normalized correspondingly. The concentrations of accumulated intermediates take this normalization into account, but the temporal development is different because the rates of consumption change slightly with biomass. The ESI‡ shows a comparison of replicate time courses that are normalized by biomass.

Modeling methods

Model design. The model was designed to analyze trehalose synthesis and degradation in non-growing cells following pulses of glucose at 30 °C or 39 °C. Because trehalose is tightly connected to glycolysis, the key components of this pathway were considered in the model (Fig. 4).

Glycolysis has been modeled for many years (*e.g.*,[22–25]), but investigations throughout the years have either omitted the trehalose branch or considered trehalose as a tangential byproduct of insignificant import (*e.g.*,[26–31]). Some metabolic modeling and simulation studies did involve trehalose dynamics, but they either did not consider heat stress[32] or translated gene expression more or less directly into enzyme activities and deduced metabolite dynamics from changes in these activities.[10,17,33] For our systems analysis, we developed a mathematical model of trehalose metabolism in the format of Generalized Mass Action (GMA) equations within the framework of Biochemical Systems Theory (BST[13–16]); details are described in the ESI.‡ The model contained twelve

dependent concentration variables and fifteen fluxes and had the format shown in eqn (1).

$$\frac{dX}{dt} = \begin{cases} -F_1/V_{ext} \\ (F_1 + 2 \cdot F_{11} - F_2)/V_{int} \\ (F_2 + F_4 - F_3 - F_9 - F_{12} - F_{15})/V_{int} \\ (F_3 - F_4 + F_6 - F_5 + F_8)/V_{int} \\ (F_5 - F_6 - F_7 - F_9)/V_{int} \\ (F_7 - F_8)/V_{int} \\ (F_9 - F_{10})/V_{int} \\ (F_{10} - F_{11})/V_{int} \\ (F_{12} - F_{13} - F_{14})/V_{int} \\ 2 \cdot F_{13}/V_{ext} \\ F_{14}/V_{int} \\ F_{15}/V_{int} \end{cases}$$

$$F = \begin{cases} B \cdot \gamma_1 \cdot \tau^{P_1} \cdot X_1^{h_1} \cdot X_3^{hr_1} \cdot Q_1^{\frac{T-30}{10}} \\ B \cdot \gamma_2 \cdot \tau^{P_2} \cdot X_2^{h_2} \cdot X_7^{hr_2} \\ B \cdot \gamma_3 \cdot \tau^{P_3} \cdot X_3^{h_3} \cdot Q_3^{\frac{T-30}{10}} \\ B \cdot \gamma_4 \cdot \tau^{P_4} \cdot X_4^{h_4} \\ B \cdot \gamma_5 \cdot \tau^{P_5} \cdot X_4^{h_5} \\ B \cdot \gamma_6 \cdot \tau^{P_6} \cdot X_5^{h_6} \\ B \cdot \gamma_7 \cdot \tau^{P_7} \cdot X_5^{h_7} \cdot X_3^{hr_3} \\ B \cdot \gamma_8 \cdot \tau^{P_8} \cdot X_6^{h_8} \cdot X_3^{hr_4} \cdot X_5^{hr_5} \\ B \cdot \gamma_9 \cdot \tau^{P_9} \cdot X_3^{h_9} \cdot X_5^{h_{10}} \cdot X_2^{hr_6} \cdot Q_9^{\frac{T-30}{10}} \\ B \cdot \gamma_{10} \cdot \tau^{P_{10}} \cdot X_7^{h_{11}} \cdot Q_{10}^{\frac{T-30}{10}} \\ B \cdot \gamma_{11} \cdot \tau^{P_{11}} \cdot X_8^{h_{12}} \cdot Q_{11}^{\frac{T-30}{10}} \\ B \cdot \gamma_{12} \cdot \tau^{P_{12}} \cdot X_3^{h_{13}} \\ B \cdot \gamma_{13} \cdot \tau^{P_{13}} \cdot X_9^{h_{14}} \cdot Q_{13}^{\frac{T-30}{10}} \\ B \cdot \gamma_{14} \cdot \tau^{P_{14}} \cdot X_9^{h_{15}} \\ 0.05 \cdot F_{12} \end{cases} \quad (1)$$

The vector dX/dt represents changes in metabolite levels X_i [mM] and F is the vector of fluxes F_i [mmol min^{-1}]. Among these, X_1 (extracellular glucose) and X_{10} (ethanol, acetate and glycerol) are measured in the medium, while the other variables, beginning with X_2 (intracellular glucose), are measured inside the cells (see Fig. 4). V_{ext} is the volume of the cell suspension and V_{int} is the total intracellular volume. B [mg of DW] is the biomass in the reactor coupled to the NMR tube, which was directly measured at the end of each experiment and found to change only modestly from one experiment to the next. The γ's are rate constants and the exponents h and hr are kinetic orders, which characterize substrate dependence and regulatory influences, respectively. The factors τ^{P_i} represent changes in protein amounts due to altered gene expression and the factors $Q_i^{\frac{T-30}{10}}$ represent the temperature dependence of the system.

Interestingly, our model analyses suggested that some of the regulatory signals discussed elsewhere[17] seemed to be very weak or non-existent in our system. A possible reason may be that our cells are in stationary phase, where apparently some of the regulatory interactions are not as significant as suggested in studies executed *in vitro*. To confirm our findings, we dedicated significant effort on more complex models that included some or all of these regulatory signals, but all fitting routines came to the conclusion that these regulatory interactions were insignificant for our datasets.

Parameter estimation. The parameters of the model consisted of three classes. First, some parameters were directly measured. The extracellular volume was V_{ext} = 50 ml. The total intracellular volume V_{int} = 7.17 ml was computed from the total biomass, B, and the yeast cell volume, *i.e.*, 2.38 µl per mg dry weight.[34,35] Specific experiments showed that the last flux in vector F, describing material entering the pentose phosphate pathway, has a magnitude of about 5% of the glycolytic flux, F_{12} (see ESI‡).

The second class of parameters consisted of the two types of quantities typical for BST models, namely rate constants γ and kinetic orders h and hr. These parameters were inferred with inverse methods from the *in vivo* NMR experiments, which produced time series data for all key metabolites (glucose, G6P, FBP, trehalose, and the end-products ethanol, acetate and glycerol) in cells of four states: control cells and heat-adapted cells, both at 30 °C and 39 °C. We posited that the intrinsic rate constants and kinetic orders, which quantify properties of enzymes, should have the same baseline values, independent of the environmental conditions.

The parameters for glucose uptake were relatively easy to characterize because glucose is the external substrate. Inspection of the glucose consumption curves (Fig. 1 and 3) suggested temperature dependence. In fact, attempts to model all uptake trends with the same kinetic parameter failed, while including a different kinetic constant for each temperature led to good representations of glucose consumption (Fig. 5).

Estimation of the remaining fluxes required optimization with the entire model. Inverse problems of this type are notoriously difficult, and we used a variety of direct and indirect methods to steer the optimization toward an acceptable solution. Some of the methods were recently reviewed in ref. 36–38. A particularly useful strategy here, as in previous estimation tasks, was the estimation of slopes from the experimental time series, which allowed us to convert the optimization task on differential equations into one exclusively using algebraic equations.[39,40]

To account for temperature dependent changes between experiments, we introduced a third class of parameters, which included temperature-induced changes in enzyme activities, Q_i, and protein abundances.

The temperature dependence was modeled as $Q_i^{\frac{T-30}{10}}$. Here Q_i are the typical temperature coefficients (Q_{10}) for enzymatic reaction i that depend on temperature (T/°C) and represent the change in enzymatic activity brought about by a 10 °C increase in temperature. The temperature actually experienced by the cells during the *in vivo* NMR experiment (30 °C or 39 °C) was explicitly included in the model as the external variable T. Q_9, Q_{10} and Q_{11} are associated with the enzymes trehalose 6-phosphate synthase, trehalose 6-phosphate phosphatase and trehalase, respectively, whose temperature profiles for activity have been reported by Neves and François.[11] We smoothed the published trends with spline functions (ESI‡ Fig. S3) for a more accurate approximation and calculated the temperature coefficients from the ratio of the enzymatic activities (R_T) between 30 °C and 39 °C, $Q_i = \left(\frac{R_{39}}{R_{30}}\right)^{\frac{10}{9}}$. No independent information was available for determining Q_1, Q_3, Q_{13}, and they were estimated from time series data as well. Furthermore, it turned out from inspection of the time courses that the glucose consumption dynamics changes with temperature. In the model, we accounted for this effect with the inclusion of a temperature-dependent kinetic order h_1.

The factors τ^{p_i} represent the changes in protein amounts due to increased gene expression, as discussed before. The values of P_i were estimated from time series together with the BST parameters; they turned out to be comparable to information found in the literature (see Results). The complete model with parameter values is presented in the ESI‡ as a file that can be copied directly into the freeware PLAS.[41]

Acknowledgements

The authors like to thank Dr Ashley Cowart of the Medical University of South Carolina for supplying the *S. cerevisiae* strain JK93dα. LLF held a fellowship (SFRH/BPD/26902/2006) from Fundação para a Ciência e a Tecnologia. The work was funded by the National Science Foundation (EOV, PI) and a grant from the University Systems of Georgia (EOV, PI). The NMR spectrometers are part of the National NMR Network (REDE/1517/RMN/2005), supported by "Programa Operacional Ciência e Inovação (POCTI) 2010" and Fundação para a Ciência e a Tecnologia (FCT). The authors have no financial interest in this work.

References

1 A. P. Gasch, P. T. Spellman, C. M. Kao, O. Carmel-Harel, M. B. Eisen, G. Storz, D. Botstein and P. O. Brown, Genomic expression programs in the response of yeast cells to environmental changes, *Mol. Biol. Cell*, 2000, **11**, 4241–57.
2 J. Postmus, A. B. Canelas, J. Bouwman, B. M. Bakker, W. van Gulik, M. J. de Mattos, S. Brul and G. J. Smits, Quantitative analysis of the high temperature-induced glycolytic flux increase in *Saccharomyces cerevisiae* reveals dominant metabolic regulation, *J. Biol. Chem.*, 2008, **283**, 23524–32.
3 Y. Ye, Y. Zhu, L. Pan, L. Li, X. Wang and Y. Lin, Gaining insight into the response logic of *Saccharomyces cerevisiae* to heat shock by combining expression profiles with metabolic pathways, *Biochem. Biophys. Res. Commun.*, 2009, **385**, 357–62.
4 L. A. Cowart, M. Shotwell, M. L. Worley, A. J. Richards, D. J. Montefusco, Y. A. Hannun and X. Lu, Revealing a signaling role of phytosphingosine-1-phosphate in yeast, *Mol. Syst. Biol.*, 2010, **6**, 349.
5 Y. A. Hannun and L. M. Obeid, Principles of bioactive lipid signalling: lessons from sphingolipids, *Nat. Rev. Mol. Cell Biol.*, 2008, **9**, 139–50.
6 T. Hottiger, P. Schmutz and A. Wiemken, Heat-induced accumulation and futile cycling of trehalose in Saccharomyces cerevisiae, *J. Bacteriol.*, 1987, **169**, 5518–22.
7 M. A. Singer and S. Lindquist, Thermotolerance in *Saccharomyces cerevisiae*: the Yin and Yang of trehalose, *Trends Biotechnol.*, 1998, **16**, 460–8.
8 C. De Virgilio, T. Hottiger, J. Dominguez, T. Boller and A. Wiemken, The role of trehalose synthesis for the acquisition of thermotolerance in yeast. I. Genetic evidence that trehalose is a thermoprotectant, *Eur. J. Biochem.*, 1994, **219**, 179–86.
9 J. M. Cherry, C. Adler, C. Ball, S. A. Chervitz, S. S. Dwight, E. T. Hester, Y. Jia, G. Juvik, T. Roe, M. Schroeder, S. Weng and D. Botstein, SGD: *Saccharomyces* Genome Database, *Nucleic Acids Res.*, 1998, **26**, 73–9.
10 E. Vilaprinyo, R. Alves and A. Sorribas, Use of physiological constraints to identify quantitative design principles for gene expression in yeast adaptation to heat shock, *BMC Bioinformatics*, 2006, **7**, 184.
11 M. J. Neves and J. François, On the mechanism by which a heat shock induces trehalose accumulation in *Saccharomyces cerevisiae*, *Biochem. J.*, 1992, **288**, 859–64.
12 A. R. Neves, A. Ramos, M. C. Nunes, M. Kleerebezem, J. Hugenholtz, W. M. de Vos, J. Almeida and H. Santos, *In vivo* nuclear magnetic resonance studies of glycolytic kinetics in *Lactococcus lactis*, *Biotechnol. Bioeng.*, 1999, **64**, 200–12.
13 M. A. Savageau, Biochemical systems analysis. I. Some mathematical properties of the rate law for the component enzymatic reactions, *J. Theor. Biol.*, 1969, **25**, 365–9.
14 M. A. Savageau, *Biochemical Systems Analysis: A Study of Function and Design in Molecular Biology*, Addison-Wesley Pub. Co. Advanced Book Program, Reading, Mass., 1976.
15 N. V. Torres and E. O. Voit, *Pathway Analysis and Optimization in Metabolic Engineering*, Cambridge University Press, New York, 2002.
16 E. O. Voit, *Computational Analysis of Biochemical Systems: A Practical Guide for Biochemists and Molecular Biologists*, Cambridge University Press, New York, 2000.
17 E. O. Voit, Biochemical and genomic regulation of the trehalose cycle in yeast: review of observations and canonical model analysis, *J. Theor. Biol.*, 2003, **223**, 55–78.
18 H. Boucherie, N. Bataille, I. T. Fitch, M. Perrot and M. F. Tuite, Differential synthesis of glyceraldehyde-3-phosphate dehydrogenase polypeptides in stressed yeast cells, *FEMS Microbiol. Lett.*, 1995, **125**, 127–33.
19 M. Marsden, R. W. Nickells, M. Kapoor and L. W. Browder, The induction of pyruvate kinase synthesis by heat shock in *Xenopus laevis* embryos, *Dev. Genet.*, 1993, **14**, 51–7.
20 R. W. Nickells and L. W. Browder, A role for glyceraldehyde-3-phosphate dehydrogenase in the development of thermotolerance in *Xenopus laevis* embryos, *J. Cell Biol.*, 1988, **107**, 1901–9.
21 L. W. Browder, M. Pollock, R. W. Nickells, J. J. Heikkila and R. S. Winning, Developmental regulation of the heat-shock response, *Dev. Biol.*, 1989, **6**, 97–147.
22 E. E. Sel'kov, Self-oscillations in glycolysis. 1. A simple kinetic model, *Eur. J. Biochem.*, 1968, **4**, 79–86.
23 T. A. Rapoport and R. Heinrich, Mathematical analysis of multienzyme systems. I. Modelling of the glycolysis of human erythrocytes, *BioSystems*, 1975, **7**, 120–129.
24 T. A. Rapoport, R. Heinrich and S. M. Rapoport, The regulatory principles of glycolysis in erythrocytes *in vivo* and *in vitro*. A minimal comprehensive model describing steady states, quasi-steady states and time-dependent processes, *Biochem. J.*, 1976, **154**, 449–469.
25 D. Garfinkel and M. J. Achs, A computer-model of the glycolytic pathway in perfused pancreatic islets, *Fed. Proc.*, 1986, **45**, 902–902.
26 J. L. Galazzo and J. E. Bailey, Fermentation pathway kinetics and metabolic flux control in suspended and immobilized *Saccharomyces cerevisiae*, *Enzyme Microb. Technol.*, 1990, **12**, 162–172.
27 R. Curto, A. Sorribas and M. Cascante, Comparative characterization of the fermentation pathway of *Saccharomyces*

cerevisiae using biochemical systems theory and metabolic control analysis. Model definition and nomenclature, *Math. Biosci*., 1995, **130**, 25–50.
28 B. Teusink, J. Passarge, C. A. Reijenga, E. Esgalhado, C. C. van der Weijden, M. Schepper, M. C. Walsh, B. M. Bakker, K. van Dam, H. V. Westerhoff and J. L. Snoep, Can yeast glycolysis be understood in terms of *in vitro* kinetics of the constituent enzymes? Testing biochemistry, *Eur. J. Biochem*., 2000, **267**, 5313–29.
29 F. Hynne, S. Danø and P. G. Sørensen, Full-scale model of glycolysis in *Saccharomyces cerevisiae*, *Biophys. Chem*., 2001, **94**, 121–163.
30 D. Bosch, M. Johansson, C. Ferndahl, C. J. Franzén, C. Larsson and L. Gustafsson, Characterization of glucose transport mutants of *Saccharomyces cerevisiae* during a nutritional upshift reveals a correlation between metabolite levels and glycolytic flux, *FEMS Yeast Res*., 2008, **8**, 10–15.
31 F. B. du Preez, R. Conradie, G. P. Penkler, K. Holm, F. L. J. van Dooren and J. L. Snoep, A comparative analysis of kinetic models of erythrocyte glycolysis, *J. Theor. Biol*., 2008, **252**, 488–496.
32 J. S. Aranda, E. Salgado and P. Taillandier, Trehalose accumulation in *Saccharomyces cerevisiae* cells: experimental data and structured modeling, *Biochem. Eng. J*., 2004, **17**, 129–140.
33 E. O. Voit and T. Radivoyevitch, Biochemical systems analysis of genome-wide expression data, *Bioinformatics*, 2000, **16**, 1023–1037.
34 G. Ditzelmüller, W. Wöhrer, C. P. Kubicek and M. Röhr, Nucleotide pools of growing, synchronized and stressed cultures of *Saccharomyces cerevisiae*, *Arch. Microbiol*., 1983, **135**, 63–7.
35 U. Theobald, W. Mailinger, M. Baltes, M. Rizzi and M. Reuss, *In vivo* analysis of metabolic dynamics in *Saccharomyces cerevisiae*: I. Experimental observations, *Biotechnol. Bioeng*., 1997, **55**, 305–16.
36 I.-C. Chou and E. O. Voit, Recent developments in parameter estimation and structure identification of biochemical and genomic systems, *Math. Biosci*., 2009, **219**, 57–83.
37 G. Goel, I.-C. Chou and E. O. Voit, System estimation from metabolic time-series data, *Bioinformatics*, 2008, **24**, 2505–11.
38 E. O. Voit, G. Goel, I.-C. Chou and L. L. Fonseca, Estimation of metabolic pathway systems from different data sources, *IET Syst. Biol*., 2009, **3**, 513–22.
39 E. O. Voit and J. Almeida, Decoupling dynamical systems for pathway identification from metabolic profiles, *Bioinformatics*, 2004, **20**, 1670–1681.
40 E. O. Voit and M. A. Savageau, Power-law approach to modeling biological systems 3. Methods of analysis, *J. Ferment. Technol*., 1982, **60**, 233–241.
41 A. E. N. Ferreira, www.dqb.fc.ul.pt/docentes/aferreira/plas.html, 1996.
42 J. L. Parrou, M. A. Teste and J. Francois, Effects of various types of stress on the metabolism of reserve carbohydrates in *Saccharomyces cerevisiae*: genetic evidence for a stress-induced recycling of glycogen and trehalose, *Microbiology*, 1997, **143**(6), 1891–900.
43 H. Zähringer, M. Burgert, H. Holzer and S. Nwaka, Neutral trehalase Nth1p of *Saccharomyces cerevisiae* encoded by the NTH1 gene is a multiple stress responsive protein, *FEBS Lett*., 1997, **412**, 615–20.